SIAM J. APPL. MATH.
Vol. 63, No. 5, pp. 1627–1647

NONLINEAR COUPLING NEAR A DEGENERATE HOPF (BAUTIN) BIFURCATION*

JONATHAN D. DROVER† AND BARD ERMENTROUT†

Abstract. A nonlinearly coupled system of bistable (fixed point and limit cycle) differential equations is analyzed. The nonlinear equations arise from the first several terms in the normal form expansion near a Bautin bifurcation. Existence and stability of in-phase and out-of-phase periodic solutions to a pair of identical systems are explored. Existence, uniqueness, and stability of traveling wave solutions from a stable rest state to a stable periodic solution are proved for the associated evolution/convolution equation. Numerical simulations suggest some interesting patterns in regimes where waves no longer exist. The results are shown to hold for a nonreduced conductance-based model.

Key words. Bautin bifurcation, subcritical Hopf bifurcation, bistability, traveling waves, localized pulses

AMS subject classifications. 37N25, 34C15, 45M99

DOI. 10.1137/S0036139902412617

1. Introduction.

The analysis of the behavior of coupled neuronal oscillators and "near" oscillators (i.e., excitable cells) has been the subject of many recent papers [2, 13, 15, 14]. Intrinsic neuronal oscillations arise primarily via two distinct mechanisms [21, 15]: (i) a saddle-node on a limit cycle bifurcation or (ii) a subcritical or supercritical Hopf bifurcation. In the saddle-node bifurcation, the oscillations that arise are large-amplitude, and so it is possible to study the effects of coupling between them by looking at certain normal forms that arise [14, 8]. Coupled systems near a supercritical Hopf bifurcation have been the subject of numerous studies (e.g., Aronson, Ermentrout, and Kopell [1]), most recently by Hoppensteadt and Izhikevich [13]. The problem with such analysis is that the coupling that has been analyzed is linear. This means that the coupling itself can determine whether or not the system is at rest or oscillates. Chemical synaptic coupling is inherently nonlinear, unlike coupling via diffusive-like interactions. This is because subthreshold oscillations and perturbations from rest are insufficient to excite the channels which release the chemical transmitters necessary for communication between neurons. Because synaptic coupling between neurons is nonlinear, the presence of coupling does not alter the stability of the resting state of such a neuron. This contrasts with diffusive or gap junctional coupling, which is linear and can therefore affect the stability of the resting state [7, 10, 19].

The oscillations emerging from a *subcritical* Hopf bifurcation generally "turn around" for neuronal models to become large-amplitude stable oscillations. Thus, like the saddle-node case, these large-amplitude oscillations are sufficient to excite chemical synapses. Furthermore, unlike a supercritical Hopf bifurcation, there is a range of parameters for which the system is intrinsically bistable: there is a stable equilibrium point and a stable oscillation. The goal of this paper is to study a reduced model (normal form) that nonlinearly couples systems with a subcritical Hopf bifurcation.

*Received by the editors August 2, 2002; accepted for publication (in revised form) February 3, 2003; published electronically July 26, 2003. Parts of this work comprised the Master's thesis for the first author. This work was supported in part by NSF grant DMS-9972913.
http://www.siam.org/journals/siap/63-5/41261.html
†Department of Mathematics, Thackeray 301, University of Pittsburgh, Pittsburgh, PA 15260 (jddst25@pitt.edu, bard@pitt.edu).

We model the bistable subcritical Hopf bifurcation by considering a degenerate form of the Hopf bifurcation, which arises at the transition between sub- and supercritical bifurcations. This is called the Bautin bifurcation, and the normal form for such a bifurcation is

$$z' = z(\lambda + b|z|^2 + f|z|^4) \equiv N(z), \tag{1.1}$$

where b, f are complex numbers and λ is the bifurcation parameter. The usual Hopf bifurcation does not involve the parameter f and is sub- or supercritical according to whether the real part of b is, respectively, positive or negative. In the Bautin bifurcation, the real part of the coefficient b vanishes. Thus, the degeneracy in the normal form arises from the nonlinear terms in the system. The advantage of the Bautin normal form is that it captures the bistability of the medium as well as the fact that the stable oscillation is bounded away from the rest state. Equation (1.1) can be derived from any nonlinear system near a degenerate Hopf bifurcation [17].

Consider, now, a pair of synaptically coupled neurons near this bifurcation. In the absence of coupling, they can be described in terms of the complex amplitudes z_1, z_2, where each z_j satisfies (1.1). Coupling alters the normal form by adding new terms, whose form can be deduced by using standard symmetry arguments [12] or by direct (albeit tedious) calculation. The coupled system has the form

$$\begin{aligned} z_1' = {} & N(z_1) + L_1 z_1 + L_2 z_2 + C_1 z_1|z_2|^2 + C_2 z_2|z_2|^2 \\ & + C_3 z_1^2 \bar{z}_2 + C_4 z_2^2 \bar{z}_1 + C_5 z_2|z_1|^2 + C_6 z_1|z_1|^2, \end{aligned} \tag{1.2}$$

with an analogous equation for z_2'. If the coupling between oscillators is through diffusion (e.g., gap junctions) then $L_1 = -L_2$. In [1, 13] only the linear coupling terms are kept. [16] studied (1.1) in the context of synchronization between bursters with linear coupling. We have also included nonlinear coupling terms up to order 3 in (1.2). The motivation for this is as follows. Consider the stability of the origin $z_j = 0$. The linearized equations have the form

$$\begin{aligned} z_1' &= (\lambda + L_1) z_1 + L_2 z_2, \\ z_2' &= (\lambda + L_1) z_2 + L_2 z_1, \end{aligned}$$

with eigenvalues $\lambda + L_1 \pm L_2$. Thus, linear coupling can alter the stability of the origin. This cannot happen in a system of synaptically coupled neurons except in very unusual circumstances. That is, the threshold for synaptic interactions would have to be nearly identical to the resting state of the neuron. For this reason, we will assume that the coupling between the two normal forms should not be linear. Thus, in this paper, we set $L_1 = L_2 = 0$.

We turn to the nonlinear coupling terms, of which there are six. Consider two neurons which are stably at rest ($z_j = 0$). Suppose that we excite one of them past threshold so that it begins to fire. Then if the neurons are coupled sufficiently strongly, this should induce the other neuron to begin firing. Of the six coupling terms in (1.2), only one term can cause this. Since $z_j = 0$ is the rest state, then any coupling term which includes z_j cannot contribute to pushing z_j away from rest. For example, if z_2 is oscillating, then the only term which can influence a *resting* z_1 is the second term:

$$z_2|z_2|^2.$$

While all terms are important once the neurons are both oscillating, the onset of oscillations is effected only through the second term. Thus, we will restrict the analysis

of coupled systems to nonlinear coupling with $C_n = 0$ except for C_2. If there is linear coupling and we are very close to the bifurcation, then the nonlinear coupling can be scaled out. Thus, one should regard our analysis, which includes nonlinear coupling terms, to hold for systems that are a small distance from the actual bifurcation. As the magnitude of the linear terms decreases (and for synaptic coupling, this is very small), the nonlinear terms have a stronger effect on the behavior, and thus in principle, we need not be very far from the critical bifurcation at all.

In the first part of the paper, we describe the bifurcations that occur in

$$\begin{aligned} z_1' &= z_1(\lambda + (iq)|z_1|^2 - |z_1|^4) + (c_1 + ic_2)z_2^2\bar{z}_2, \\ z_2' &= z_2(\lambda + (iq)|z_2|^2 - |z_2|^4) + (c_1 + ic_2)z_1^2\bar{z}_1, \end{aligned} \tag{1.3}$$

where $b = iq$ (at the Bautin bifurcation) and all parameters are real. We restrict our attention to the case in which the coefficient f in (1.1) is real and negative since we want the resulting large-amplitude oscillations to be stable. We set $f = -1$ with no loss in generality. We establish the existence and stability of in- and out-of-phase oscillations in preparation for section 3 in which we look at spatially distributed networks.

Spatially distributed neurons and waves have been the object of much recent analysis. Coupling between neurons is not restricted to nearest neighbors but instead can involve long spatial scales. Typically, when modeled as a continuum, interactions take the form of convolutions. The coupled pair of Bautin oscillators can be easily generalized to a continuous spatial model with convolution coupling:

$$z_t = z(\lambda + (iq)|z|^2 - |z|^4) + (c_1 + ic_2)\int_{-\infty}^{\infty} J(x-y)z^2(y)\bar{z}(y)dy. \tag{1.4}$$

In the second part of the paper, we will describe the existence of traveling wavefronts, which join the stable resting state to an oscillatory solution. The resulting waves are similar in structure to those found in [9] when coupling was diffusive. We analyze the existence and stability of plane waves for (1.4) as well. We use numerical simulations to find spatially localized patterns which may be analogous to patterns of activity used to model working memory. Finally, we close the paper with simulations of a simple biophysically based model in order to demonstrate that the behavior of the normal-form-based model holds in more "realistic" neural models.

2. Two coupled equations. In this section we determine under what conditions the symmetric and asymmetric solutions exist and are stable. For this analysis, it is easiest to put the equations into polar form. We let

$$z_j = r_j e^{i\theta_j}$$

and let $\phi = \theta_1 - \theta_2$. Then, substituting into (1.3), we obtain the equations

$$\begin{aligned} r_1' &= \lambda r_1 - r_1^5 + c_1 r_2^3\cos(\phi) + c_2 r_2^3\sin(\phi), \\ r_2' &= \lambda r_2 - r_2^5 + c_1 r_1^3\cos(\phi) - c_2 r_1^3\sin(\phi), \\ \phi' &= q(r_1^2 - r_2^2) - c_1\left(\frac{r_1^3}{r_2} + \frac{r_2^3}{r_1}\right)\sin(\phi) + c_2\left(\frac{r_2^3}{r_1} - \frac{r_1^3}{r_2}\right)\cos(\phi). \end{aligned} \tag{2.1}$$

Phase-locked solutions with constant r_1, r_2 to the coupled system of oscillators are fixed points of (2.1). The existence and stability of periodic solutions is readily obtained. We remark that $z_j = 0$ is an asymptotically stable solution to (1.3) if and only

if $\lambda < 0$. In this section, we will look for limit-cycle solutions to (1.3) with amplitudes r_j bounded away from zero so that the denominators in the equation for ϕ cause no problems.

2.1. Symmetric in-phase solutions. We look for solutions of the form $\rho = r_1 = r_2$ (symmetric) and $\phi = 0$. When $\phi = 0$, the sine terms in (2.1) vanish. Inserting the solution $\phi = 0$, (2.1) is reduced to the first order ODE

$$\rho' = \lambda\rho + c_1\rho^3 - \rho^5. \tag{2.2}$$

The positive roots are given by

$$\frac{1}{2}\sqrt{2c_1 \pm 2\sqrt{c_1^2 + 4\lambda}}. \tag{2.3}$$

First, we will establish when these solutions exist.

2.1.1. Existence. We want to determine under what conditions on the parameters the solutions (2.3) are real. Thus we want to know when the polynomial $f(x) = \lambda + c_1x^2 - x^4$ has two positive, real roots. For $\lambda > 0$ this polynomial will always have one positive root; thus the upper branch of solutions (2.3) will be real. Now, because this polynomial is symmetric about the y-axis, in order for two real, positive roots to exist it must be true that $f(0) < 0$, implying $\lambda < 0$. Also, there must be a relative maximum at a point $x = a$ so that $f(a) > 0$. This maximum occurs at $x = \sqrt{c_1/2}$. Thus, the polynomial $f(x)$ will have two positive, real roots if $c_1 > \sqrt{-2\lambda}$.

One of the goals of this paper is to prove the existence of traveling waves connecting a stable rest state to a stable plane wave. Thus, we must choose parameters so that equations lie in a bistable regime. For this reason, we will only consider parameter values that allow two stable states. Thus, we must have two nonzero solutions to separate stable regions. We will consider only $\lambda < 0$. The only requirement that follows is that $c_1 > \sqrt{-2\lambda}$ must hold.

2.1.2. Stability. The Jacobian for the polar coordinate system is

$$\begin{pmatrix} \alpha(r) & \beta(r) & \gamma(r) \\ \beta(r) & \alpha(r) & -\gamma(r) \\ a(r) & -a(r) & b(r) \end{pmatrix}, \tag{2.4}$$

where $\alpha(r) = \lambda - 5r^4$, $\beta(r) = 3c_1r^2$, $\gamma(r) = c_2r^2$, $a(r) = 2qr - 4c_2r$, and $b(r) = -2c_1r^2$.

The characteristic polynomial for (2.4) is

$$(x - \alpha - \beta)(x^2 + (\beta - b - \alpha) + \alpha b - \beta b - 2\gamma a).$$

Thus, a symmetric in-phase solution is stable if the following three conditions hold at the equilibrium:

$$\alpha + \beta < 0, \tag{2.5}$$

$$\beta - b - \alpha > 0, \tag{2.6}$$

$$\alpha b - \beta b - 2\gamma a > 0. \tag{2.7}$$

The lower branch of solutions is always unstable. Substituting the value of the lower branch solution into $\alpha + \beta$ gives

$$-4\lambda - c_1^2 + c_1\sqrt{c_1^2 + 4\lambda}.$$

By the requirement for existence, we have that $c_1 > \sqrt{-2\lambda}$, and so the above quantity is real. It is easily seen that the expression is the same as

$$\sqrt{c_1^2 + 4\lambda}\left[c_1 - \sqrt{c_1^2 + 4\lambda}\right] > 0,$$

and so the value (2.5) is positive. Thus this periodic solution to (2.2) is unstable and will act as the desired separatrix between the stable fixed point and the upper periodic branch. A similar proof is used to show that this eigenvalue is always negative for the upper branch of solutions; thus it will not prevent stability.

We turn now to the other two conditions. First, consider condition (2.6). Using the definitions of the various parameters, this condition becomes

$$5c_1^2 + 4\lambda + 5c_1 R > 0,$$

where $R = \sqrt{(c_1^2 + 4\lambda)} > 0$. Since $c_1^2 + 4\lambda > 0$, this expression is clearly positive, and thus the condition (2.6) holds on the upper branch. The last condition, (2.7), will not hold for all parameters, and in fact, as we will show, the left-hand side can become negative if the parameters c_2, q are sufficiently large. We can rewrite condition (2.7) as

$$F(c_2) \equiv Ac_2^2 + Bc_2 + C > 0,$$

where

$$\begin{aligned} A &= 4c_1^2 + 8\lambda + 4c_1 R, \\ B &= -q(c_1^2 + 4\lambda + c_1^2 + c_1 R) \equiv -qD, \\ C &= 4c_1 R(\lambda + 2c_1^2) + 4c_1^2(5\lambda + 2c_1^2). \end{aligned}$$

We note that since $c_1^2 + 4\lambda > 0$, $\lambda < 0$, and $c_1 > 0$, A, D, C are all positive. In particular, if $c_2 = 0$, then condition (2.7) holds and the upper branch is asymptotically stable. Suppose that c_2 is nonzero. The parameter q appears only in the coefficient B. Furthermore, $D > 0$ so that for fixed c_2 we can always find a sufficiently large value of $|q|$ so that $F(c_2) < 0$ and the upper branch is destabilized. We should choose c_2, q to have the same sign. The critical value of q leads to a zero eigenvalue for the stability matrix. Since the synchronous solution cannot disappear (its existence is independent of both c_2, q), the bifurcation occurring must be either a transcritical or a pitchfork. However, due to symmetry, the transcritical cannot occur, and the resulting bifurcation must be a pitchfork [23]. The critical value of q is readily found to be

$$q^* = \frac{Ac_2^2 + C}{Dc_2}.$$

Using AUTO [6], we have tracked the solution through this instability and verified that it is indeed a pitchfork bifurcation. For $\lambda = -1/5$, $c_1 = c_2 = 1$, we find that the synchronous state becomes unstable at $q^* = 5.4473$, in agreement with the above formula. Furthermore, the bifurcation is subcritical. Thus, once the critical value of q is exceeded, we find that the only stable state is the resting value, $r_1 = r_2 = 0$.

2.2. Symmetric out-of-phase solutions. In order for the out-of-phase solutions to exist we must have that $c_1 < 0$. In this paper we will assume that $c_1 > \sqrt{-2\lambda}$ and $\lambda < 0$, so these solutions are of little interest here.

2.3. Two-equation summary. For $\lambda < 0$ and $c_1 > \sqrt{-2\lambda}$ there are two in-phase symmetric periodic solutions. The top branch of solutions is stable as long as q is sufficiently small. The lower branch is unstable. These solutions, and the zero solution which is linearly stable, provide a bistable region. For the two-equation system this is of little consequence in the existence and stability of phase-locked periodic solutions; however, when modeled in continuum, the bistability leads to traveling waves and pulsing behaviors that connect the stable origin to the stable periodic solutions, as we shall see in the subsequent sections.

3. The convolution equation. As stated in the introduction, we will consider the equation

$$z_t = z[\lambda + (b_1 + iq)|z|^2 - |z|^4] + (c_1 + ic_2)\int_{-\infty}^{\infty} J(x-y)z^2(y)\overline{z}(y)dy,$$

where $\int_{-\infty}^{\infty} J(x)dx = 1$, $J(x) \geq 0$, and $||J||_\infty < \infty$. We remark that if $c_2 = 0$, then, no matter what the value of q, the synchronous periodic state $z(x,t) = \rho \exp(i\Omega t)$ is always stable when it exists. We will also assume that $b_1 \geq 0$ since we want the local Hopf bifurcation to be subcritical (and, in fact, throughout most of the paper, we assume $b_1 = 0$). We will first study the existence and stability of plane wave solutions to this system. We then turn to the existence of traveling fronts, which join the stable equilibrium point, $z = 0$, to a plane wave. Finally, we look at the behavior of these fronts as q increases. We present numerical evidence for the existence of localized regions of periodic activity surrounded by the near absence of activity.

3.1. Relationship of the normal form to a kinetic model. The relationship between the coupling in an actual kinetic model and the normal form given in (1.4) is derived here. Consider the following system consisting of two synaptically coupled neurons:

$$\begin{aligned}
\frac{dV_1}{dt} &= f(V_1) - gs_2(V_1 - V_{syn}),\\
\frac{ds_1}{dt} &= \alpha(V_1)(1-s_1) - \beta s_1,\\
\frac{dV_2}{dt} &= f(V_2) - gs_1(V_2 - V_{syn}),\\
\frac{ds_2}{dt} &= \alpha(V_2)(1-s_2) - \beta s_2.
\end{aligned}$$

Assume that $f(V_{rest}) = 0$ and that $\frac{\partial f}{\partial V}(V_{rest}) < 0$. Then the uncoupled system has a stable rest state at $V = V_{rest}$. Suppose that $\alpha(V) = \alpha'(V) = 0$ for V less than some critical value, which itself is greater than V_{rest}. Then V_{rest} will remain a stable equilibrium point for the coupled system. Hence, the coupling will not affect the existence or stability of the rest state. If we consider N neurons coupled similarly, we get a system

$$\begin{aligned}
\frac{dV_i}{dt} &= f(V_i) - g(V_i - V_{syn})\sum_j w_{i-j}s_j,\\
\frac{ds_i}{dt} &= \alpha(V_i)(1-s_i) - \beta s_i.
\end{aligned}$$

We may slave the coupling directly to the presynaptic potentials. Because we have that $\alpha(V_{rest}) = \alpha'(V_{rest}) = 0$, the expression must be at least second order, and we

get that

$$\frac{dV_i}{dt} = f(V_i) - g(V_i - V_{syn}) \sum_j w_{i-j} R(V_j - V_{rest}),$$

where R is a function with no linear component. Because we are allowing only terms that contribute to excitation away from rest, we may simplify even further:

$$\frac{dV_i}{dt} = f(V_i) - g(V_{rest} - V_{syn}) \sum_j w_{i-j} R(V_j - V_{rest}).$$

And finally, if modeled in continuum, we get that

$$V_t(x,t) = f(V(x,t)) - \hat{g} \int_{\infty}^{\infty} J(x-y) R(V(y,t) - V_{rest}) dy,$$

as desired. (Note that $\hat{g} = g(V_{rest} - V_{syn})$.)

3.2. Plane wave solutions. Consider solutions of (1.4) of the form $\rho e^{i(\Omega t - kx)}$. Substituting this in yields

$$\begin{aligned} i\rho\Omega e^{i(\Omega t-kx)} &= \rho e^{i(\Omega t-kx)}(\lambda + (b_1 + iq)\rho^2 - \rho^4) \\ &\quad + (c_1 + ic_2)\int_{-\infty}^{\infty} J(x-y)\rho^3 e^{i(\Omega t - ky)} dy, \end{aligned}$$

which implies

$$i\Omega = \lambda + (b_1 + iq)\rho^2 - \rho^4 + \rho^2(c_1 + ic_2)\int_{-\infty}^{\infty} J(x-y)e^{ik(x-y)} dy$$

and finally

$$i\Omega = \lambda + (b_1 + iq)\rho^2 - \rho^4 + \rho^2(c_1 + ic_1)\hat{J}(k), \tag{3.1}$$

where $\hat{J}(k) = \int_{-\infty}^{\infty} J(s)e^{iks} ds$. Taking the imaginary part of the right-hand side of (3.1), we find that

$$\Omega = q\rho^2 + c_1\rho^2 \mathrm{Im}(\hat{J}(k)) + c_2\rho^2 \mathrm{Re}(\hat{J}(k)), \tag{3.2}$$

with ρ determined so that

$$\lambda + b_1\rho^2 - \rho^4 + c_1\rho^2 \mathrm{Re}(\hat{J}(k)) - c_2\rho^2 \mathrm{Im}(\hat{J}(k)) = 0. \tag{3.3}$$

For the remainder of the paper, we will assume that $c_2 = 0$ and that $J(x)$ is a symmetric kernel; thus (3.2) and (3.3) become, respectively,

$$\Omega = q\rho^2 \tag{3.4}$$

and

$$\lambda - \rho^4 + c_1\rho^2 \hat{J}(k) = 0. \tag{3.5}$$

In the next subsection, we prove the asymptotic stability of these plane waves so that we can then show the existence of traveling wavefronts connecting the stable rest state to these oscillations. We remark that setting $c_2 = 0$ is a major simplification. It is well known that if $c_2 q$ is large enough, then the corresponding Ginzburg–Landau model has spatiotemporal chaos. (See, for example, [20], where spatiotemporal chaos is explored for $z_t = z(a + bz\bar{z}) + dz_{xx}$. See also section 3.4.3, where such a solution is exhibited for the present model.)

3.3. Plane wave stability. We claim that the plane wave solutions defined by (3.5), (3.4) are asymptotically stable for sufficiently small k. We will show this using a symmetric kernel $J(x)$ such that $\frac{dJ}{dx}(0) = 0$ and $\int_{-\infty}^{\infty} J(x)dx = 1$. The kernel we use is $(1/\sqrt{\pi})e^{-x^2}$, and the results can be generalized to any function satisfying the above requirements.

The plane wave has the form $z(x,t) = \rho e^{i(\Omega t - kx)}$, with ρ and Ω defined as in (3.5) and (3.4). We now examine the stability of the plane waves by linearizing about a solution. Let

$$z(x,t) = \rho e^{i(\Omega t - kx)} + w(x,t). \tag{3.6}$$

Substituting (3.6) into (1.4) and taking terms linear in w, we obtain

$$w_t = f(w) + c_1\rho^2 \int_{-\infty}^{\infty} J(x-y)\left[e^{2i(\Omega t - kx)}\bar{w} + 2w\right] dy, \tag{3.7}$$

where

$$f(w) = \lambda w + iq\rho^2\left[2w + e^{2i(\Omega t - kx)}\bar{w}\right] - \rho^4\left[3w + 2e^{2i(\Omega t - kx)}\bar{w}\right]. \tag{3.8}$$

Now, let $w = e^{i(\Omega t - kx)}v$ and $v = v_1 + iv_2$ and substitute into (3.7). This gives the equation

$$\begin{aligned} i\Omega(v_1 + iv_2) + (v_1 + iv_2)_t \\ = g(v_1, v_2) + c_1\rho^2 \int_{-\infty}^{\infty} J(s)e^{iks}\left[3v_1(x-s) + iv_2(x-s)\right] ds, \end{aligned} \tag{3.9}$$

where

$$g(v) = \lambda(v_1 + iv_2) + 2iq\rho^2(v_1 + iv_2) + iq\rho^2(v_1 - iv_2) - 3\rho^4(v_1 + iv_2) - 2\rho^4(v_1 - iv_2).$$

Expanding the integrand in (3.9) and separating the real and imaginary parts gives

$$c_1\rho^2 \int_{-\infty}^{\infty} J(s)\left[3\cos(ks)v_1(x-s) - \sin(ks)v_2(x-s)\right] ds \tag{3.10}$$

and

$$c_1\rho^2 \int_{-\infty}^{\infty} J(s)\left[\cos(ks)v_2(x-s) + 3\sin(ks)v_1(x-s)\right] ds. \tag{3.11}$$

Let $g = g_1 + ig_2$. Then these are

$$g_1(v) = \lambda v_1 - q\rho^2 v_2 - 5\rho^4 v_1 \tag{3.12}$$

and

$$g_2(v) = \lambda v_2 + 3q\rho^2 v_1 - \rho^4 v_2. \tag{3.13}$$

Because $\Omega = q\rho^2$, we can subtract this from both sides of (3.9). We define

$$h_1(v) = g_1(v) + q\rho^2 v_2 = \lambda v_1 - 5\rho^4 v_1, \tag{3.14}$$

$$h_2(v) = g_2(v) - q\rho^2 v_1 = \lambda v_2 + 2q\rho^2 v_1 - \rho^4 v_2. \tag{3.15}$$

Now, let $v_1 = e^{\alpha t}e^{ilx}u_1$ and $v_2 = e^{\alpha t}e^{ilx}u_2$. Then (3.10) becomes

$$c_1\rho^2 e^{\alpha t}e^{ilx}\int_{-\infty}^{\infty} J(s)\left[3\cos(ks)e^{-ils}u_1 - \sin(ks)e^{-ils}u_2\right]ds,$$

which, because J is assumed to be even, simplifies to

$$c_1\rho^2 e^{\alpha t}e^{ilx}\left[3\int_{-\infty}^{\infty} J(s)\cos(ks)\cos(ls)u_1 ds + \int_{-\infty}^{\infty} J(s)\sin(ks)\sin(ls)u_2 ds\right]. \tag{3.16}$$

Similarly, (3.11) becomes

$$c_1\rho^2 e^{\alpha t}e^{ilx}\left[\int_{-\infty}^{\infty} J(s)\cos(ks)\cos(ls)u_2 ds - 3\int_{-\infty}^{\infty} J(s)\sin(ks)\sin(ls)u_1 ds\right]. \tag{3.17}$$

Thus, (3.9) becomes

$$\alpha u_1 = \left[\lambda - 5\rho^4 + 3c_1\rho^2 J_{cc}\right]u_1 + iJ_{ss}u_2, \tag{3.18}$$

$$\alpha u_2 = \left[\lambda - \rho^4 + c_1\rho^2 J_{cc}\right]u_2 + \left[2q\rho^2 - iJ_{ss}\right]u_2, \tag{3.19}$$

where

$$J_{ss} = \int_{-\infty}^{\infty} J(s)\sin(ks)\sin(ls)ds$$

and

$$J_{cc} = \int_{-\infty}^{\infty} J(s)\cos(ks)\cos(ls)ds.$$

These can be expressed in terms of the Fourier transform $\hat{J}(k)$ of the kernel

$$J_{cc} = \frac{1}{2}\hat{J}(k+l) + \frac{1}{2}\hat{J}(k-l)$$

and

$$J_{ss} = -\frac{1}{2}\hat{J}(k+l) + \frac{1}{2}\hat{J}(k-l).$$

For the kernel J chosen, we have the transform $\hat{J}(k) = e^{-\frac{1}{4}k^2}$. The top panel of Figure 1 shows that, for $k = 0$, the real part of the greatest eigenvalue is negative for all $l \neq 0$. The middle panel shows that when $k = 1$, the plane wave solution is unstable, with the real part of the greatest eigenvalue positive. The bottom panel shows that there is a $k > 0$ such that the corresponding plane wave is stable. Thus there is an interval surrounding $k = 0$ such that the perturbation goes to zero, and hence the plane wave is stable.

This result is generalizable to any symmetric, nonnegative, integrable kernel qualitatively like a Gaussian. We need only that $\hat{J}$ decreases as $|k|$ gets farther from 0.

3.4. Traveling wavefronts. We will show that, under certain restrictions on the parameters, there exists a traveling wavefront that takes the system from the stable equilibrium point $z = 0$ to the plane wave solutions defined by (3.4), (3.5).

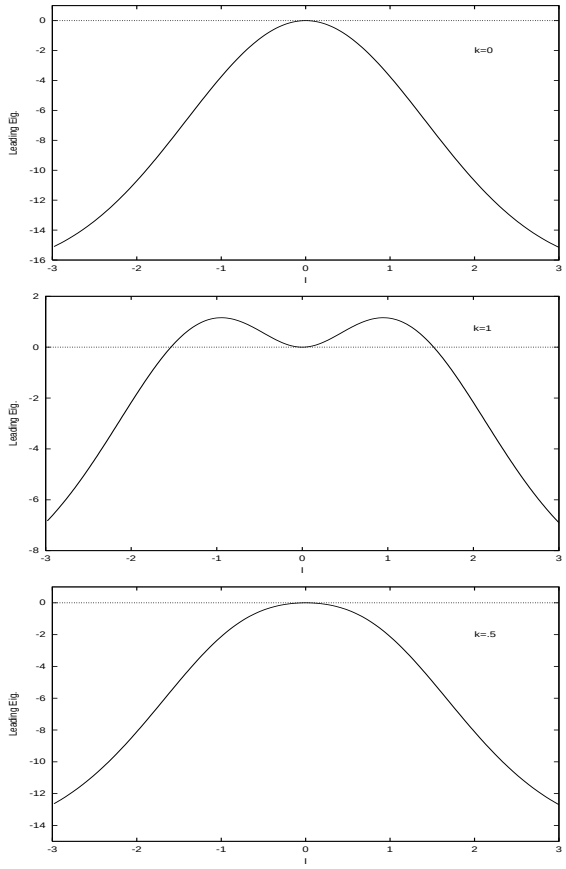

FIG. 1. *The real part of the leading eigenvalue for $k = 0$, $k = 1$, and $k = .5$. The horizontal axis is l, and the vertical axis is the value of the real part of the eigenvalue.*

Let $Z(k; x, t) = \rho(k) \exp(i[\Omega(k)t - kx])$ be a plane wave as constructed above. For $k = k^*(q)$ we seek traveling waves connecting $z(x, t) = 0$ to $Z(k^*; x, t)$. That is, there exists a real valued function $h(\xi)$ and a real c such that

$$z(x, t) = h(x - ct)Z(k^*; x, t),$$

where $h(-\infty) = 0$ and $h(\infty) = 1$. In this paper, we prove only the $q = 0$ case.

We put the system (1.4) into polar coordinates, making the substitution $z = re^{i\theta}$:

$$r_t = \lambda r + b_1 r - r^5 + c_1 G_1(x, t) + c_2 G_2(x, t), \tag{3.20}$$

$$r\theta_t = qr^3 + c_1 G_2(x, t) + c_2 G_1(x, t), \tag{3.21}$$

where

$$G_1(x, t) = \int_{-\infty}^{\infty} J(x - y)r^3(y)\cos(\theta(x) - \theta(y))dy, \tag{3.22}$$

$$G_2(x, t) = \int_{-\infty}^{\infty} J(x - y)r^3(y)\sin(\theta(x) - \theta(y))dy.$$

First, suppose that $b_1 = q = c_2 = 0$. Then $\theta = 0$ satisfies (3.21). This makes (3.20)

$$\rho' = \lambda\rho + b_1\rho^3 - \rho^5 + c_1 \int_{-\infty}^{\infty} J(x-y)\rho^3(y)dy. \tag{3.23}$$

3.4.1. Existence, uniqueness, asymptotic stability. Proving the existence, uniqueness, and asymptotic stability of a traveling wave connecting the stable equilibrium at $z = 0$ with a stable periodic orbit is done by appealing to the following theorem.

THEOREM 3.1 (see Chen [4]). *Consider the evolution equation*

$$u_t = Du_{xx} + G(u, J_1 * S_1(u), \ldots, J_n * S_n(u)), \tag{3.24}$$

where $J*S(u)$ stands for the convolution $\int_R J(x-y)S(u(y))dy$. Assume the following:

1. *For some $a \in (0,1)$, the function $f(u) = G(u, S_1(u), \ldots, S_n(u))$ satisfies $f > 0$ in $(-1,0) \cup (a,1)$, $f < 0$ in $(0,a) \cup (1,2)$, and $f'(0) < 0$, $f'(a) > 0$, and $f'(1) < 0$.*

2. *For each $i = 1, \ldots, n$, the kernel J_i is C^1 and satisfies $J_i(.) \geq 0$, $\int_R J_i(y)dy = 1$, and $\int_R |J_i(y)|dy < \infty$.*

3. *The functions $G(u,p)$ ($p = (p_1, \ldots, p_n)$) and $S_1(u), \ldots, S_n(u)$ are smooth functions satisfying for all $u \in [-1,2]$, $p \in [-1,2]^n$, $i = 1, \ldots, n$, $G_{p_i}(u,p) \geq 0$, $S_{u_i}(u) \geq 0$.*

4. *Either $D > 0$ or $G_u(u,p) < 0$ and $G_{p_1}(u,p)S_{u_1}(u) > 0$ on $[-1,2]^{n+1}$.*

If conditions 1–4 hold, there exists a unique (up to a translation) asymptotically stable, monotone traveling wave connecting 0 to 1.

Remark. In our system, the fixed point $\rho = 0$ corresponds to the zero fixed point of (1.4), and the fixed point $\rho > 0$ corresponds to the synchronous periodic solution to (1.4). Here $k^*(0) = 0$.

We now show that the following assumptions hold for (3.23).

1. The function $f(x) = \lambda x + b_1x^3 - x^5 + c_1x^3$ must satisfy a number of conditions regarding stability. This is to ensure that there is both a stable equilibrium and a stable periodic solution with an unstable periodic solution between the two acting as a separatrix. The first condition is $f(0) = 0$, $f(a) = 0$, and $f(b) = 0$, where b is the amplitude of the stable periodic orbit and a is the amplitude of the unstable separatrix. These values can be scaled so that $b = 1$; however, that is not necessary to satisfy the assumption. The requirements that $f'(0) < 0$ and $f'(b) < 0$ are simply to ensure that both the rest state and periodic solution are stable solutions. $f(x)$ does satisfy these conditions, as shown in section 1.2, so the first assumption in Chen's theorem is satisfied.

2. $\int_{-\infty}^{\infty} J(x-y)dy = 1$, $J(x) \geq 0$, and $J(x)$ is bounded for all x. We defined J in this way, so this assumption is satisfied.

3. $G_p(u,p) > 0$. For our purposes, this quantity is just c_1, so we will assume $c_1 > 0$. This is necessary for the existence of a nonzero root for f.

4. $G_u(u,p) < 0$ and $S_u(u) > 0$. The first of these is true for sufficiently small b_1. Because we have assumed that $b_1 = 0$, this condition is satisfied. The second quantity, $3c_1u^2$, is slightly problematic because it vanishes at $u = 0$; however, because it holds for all $u \neq 0$, the inequality that this condition is used to satisfy is still satisfied for our purposes (see the proof of Chen's theorem). Hence, this assumption is satisfied.

Because all four of the assumptions are valid for the scalar equation, there exists a unique and asymptotically stable traveling wave connecting the stable fixed point at $z = 0$ and the stable periodic solution of (3.23).

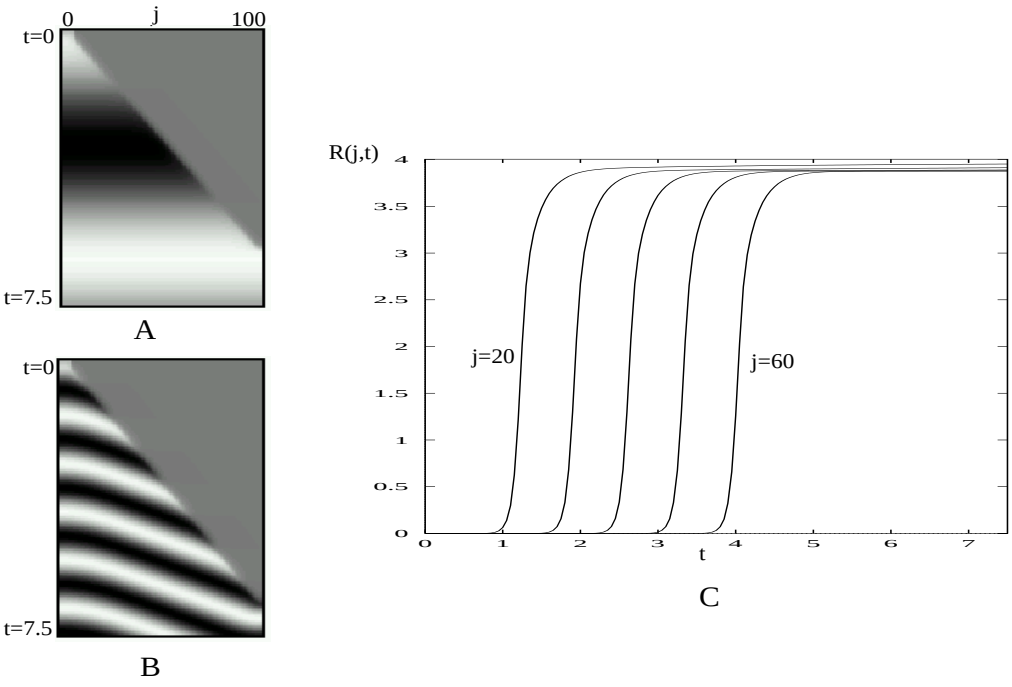

FIG. 2. *Traveling wave solution.* (A) $q = 0.0$, $\lambda = -0.2$, $c_1 = 1$. *This shows* $u(j,t)$ *with* j *horizontal and* t *vertical. Lightest color is* $u = 2$*, and darkest,* $u = -2$. (B) *Same as* (A) *but* $q = 1.0$. (C) *Amplitude* $R = u^2 + v^2$ *as a function of* t *for* $j = 20, 30, 40, 50, 60$*, for* $q = 1.0$.

Since $\theta = 0$, the imaginary part of z is never excited; hence the wave propagated will be from the stable solution $z(x) = 0$ for all $x > x_0$ (without loss of generality we may assume that the wave propagates from left to right) to the stable (parameter dependent) periodic $z(x) = \rho_0$ with zero imaginary part, as shown in Figure 2(A). There is no phase-gradient; all of the oscillators are perfectly synchronized after the wave passes. Because there is no imaginary component of the wave, it has wave number 0. Although we have no proof of existence of the wave for nonzero q, we expect that waves continue to exist at least for some finite range of q around 0. Figure 2(B,C) shows a simulation of the equations for $q = 1.0$. The magnitude, $R = u^2 + v^2$, travels as a front, but there is a clear phase-gradient in the wake of the wave. The frequency of the oscillations is also higher. More properties of the case $q \neq 0$ are considered in the next section.

3.5. The parameter q.

3.5.1. Small q. Assume that $b_1 = c_2 = 0$ and that q is sufficiently small. (Here, small depends on the parameters λ and c_1.) For nonzero q, we cannot assume that $\theta = 0$, so that a phase-gradient will appear (see Figure 2(B)). This, in turn, lowers the effective coupling strength between the oscillators since the coupling includes the term $\cos(\theta(y) - \theta(x))$, and for a large enough gradient, this can be quite small. Thus, one effect of increasing q is the appearance of a phase-gradient which, in turn, weakens the effective coupling strength and thus should slow the wave down.

Figure 3 shows some properties of the wavefront as a function of the magnitude q for $\lambda = -0.2, c_1 = 1$ fixed. As expected from the above discussion, the parameter q

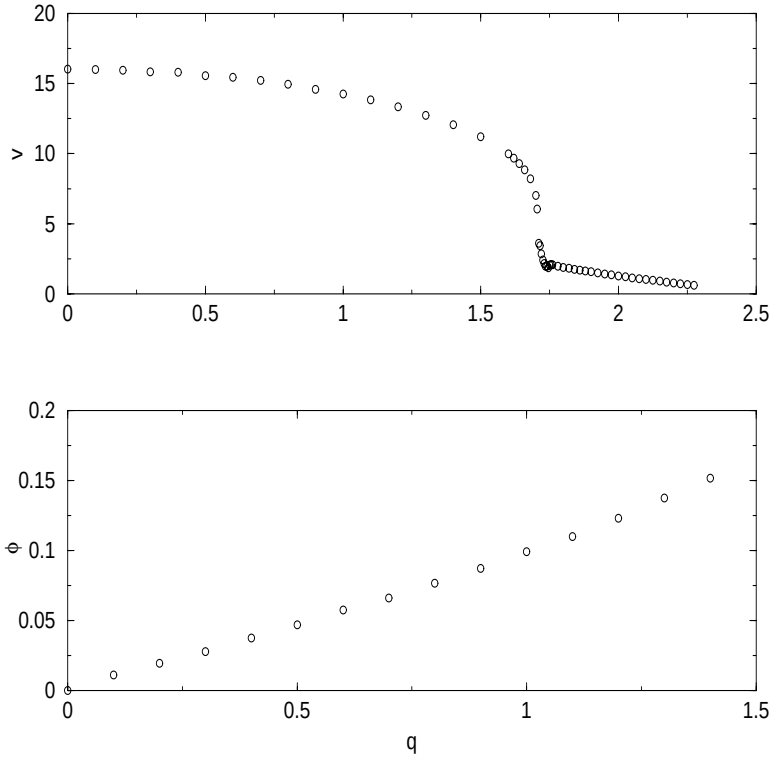

FIG. 3. *Dependence of the wave properties on the parameter q. Upper panel shows the velocity of the front for* $\lambda = -0.2$ *and* $c_1 = 1$. *Lower panel shows the phase-gradient. Note the different horizontal scales. The simulation consists of* 100 *cells coupled to* 20 *nearest neighbors with coupling strength* $\exp(-|j|/2)$. *Front velocity is measured as follows. Let* T_j *denote the time at which* $r_j = 1$. *Then the plotted velocity is just* $10/(T_{70} - T_{60})$, *that is,* $\Delta x/\Delta t$. *The phase-gradient is measured as follows. Let* $\theta_j = \arctan(v_j/u_j)$. *The quantity* $D(t) = (\theta_{60} - \theta_{40})/20 \approx \theta_x$ *is plotted, and the value after the second oscillation is taken to be an approximation of the phase gradient. In a finite domain,* $D(t)$ *always goes to zero since the network synchronizes.*

slows the wave down. For low values of q, this is a gradual decrease in speed. However, at $q \approx 1.75$ there is a precipitous drop in the velocity. For q larger than about 2.25, the wave ceases to exist and is replaced by a stable localized pulse (see below). The critical value of q depends on both the coupling strength c_1 and λ. The closer λ is to zero, the less excitation is required to cause propagation, due to the location of the unstable periodic orbit separating the rest state from the stable oscillation. Thus, for λ close to zero, wave propagation can occur for higher values of q. As λ gets larger in magnitude, the separatrix is farther from the stable rest state, and propagation of a wavefront requires more from the coupling, which large q prevents. This means that if q is fixed, we can achieve a similar slowing by altering the parameter λ. Indeed, we will exploit this in the next section, where we show similar phenomena for a conductance-based neural model. In addition to the drop in the velocity, the phase-gradient increases with q in an almost linear fashion. We compute the phase-gradient only up to about $q = 1.4$, as beyond that, the wave velocity becomes nearly zero, and whether or not there is a traveling front becomes ambiguous. The nearly linear dependence on q leads to a simplification for analyzing the effects of q on the wave velocity. Assume that the oscillations behind the front are quickly drawn to the plane

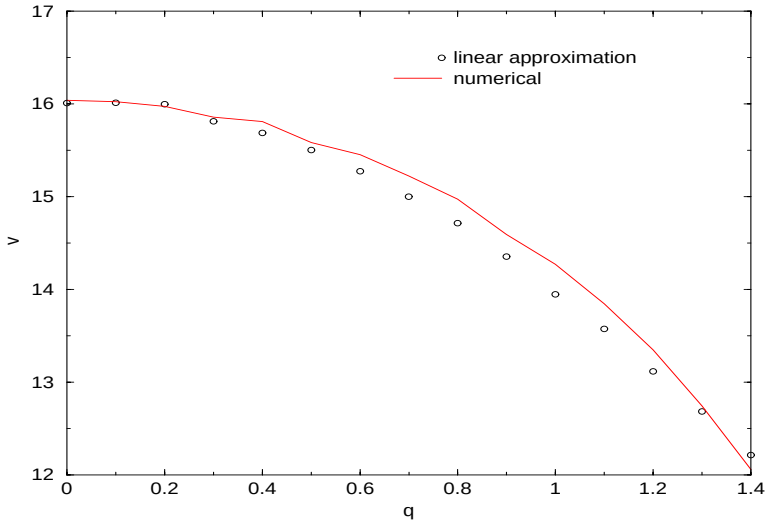

FIG. 4. *Velocity of the full equations (Figure* 3*, top) as* q *varies compared to the velocity computed from the approximate equation* (3.25) *using* $k(q) = q/10$*, which approximates the slope of the lower curve in Figure* 3.

wave and thus $\theta(x,t) = \Omega t + k(q)x$. Here $k(q) \approx mq$ is the asymptotic wave number, and m is the slope of the dependence. Then the amplitude evolves according to the equation

$$r_t = r(\lambda + b_1 r^2 - r^4) + c_1 \int_{-\infty}^{\infty} \tilde{J}(x-y) r^3(y)\, dy, \tag{3.25}$$

where $\tilde{J}(x) = J(x)\cos(k(q)x)$. This is identical (up to normalization) to the zero q model, for which we have proved the existence of a front. Thus, we expect that there will continue to be traveling fronts for q small enough. However, the new convolution kernel $\tilde{J}$ is narrower than the original, and thus we expect the velocity to decrease. Figure 4 shows a comparison of the front velocity for the approximation and the full equations. For values up to $q \approx 1.4$ the approximation is very good. (Recall that the computation of the phase became difficult beyond $q = 1.4$.) For larger values of q, the approximation was not very good.

3.5.2. Larger q and pulse formation. We saw above that the velocity of the front seems to go to zero as q approaches some fixed finite value. We can ask what happens for q beyond this point. One possibility is that the wave will not propagate at all and all initial data will return to the rest state, $z = 0$. However, numerical simulations indicate that rather than decay to rest, the medium remains excited locally and forms localized pulses. Because this excitation is necessary to get the θ variable excited, q large will prohibit excitation. The parameters are selected to lie in a bistable region, and thus the solution $z(t,x) = 0$ is stable. If there is not sufficient coupling, the wave will not propagate, and under sufficiently large initial conditions this can result in bumps or pulse solutions (see Figure 5). This figure shows the real part $u(x,t)$ in a simulation for $q = 3.25$, which is past the regime of existence of traveling fronts. The envelope $R = u^2 + v^2 = |z|^2$ of a pulse appears to be stationary (inset, Figure 5(B)), while the imaginary part appears to be periodic.

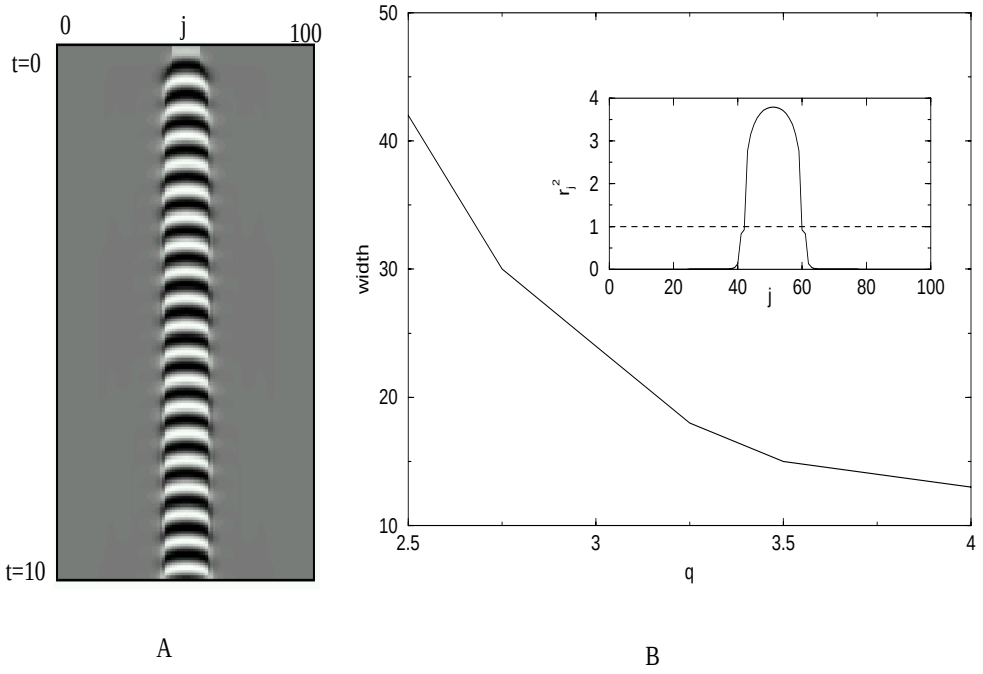

FIG. 5. (A) *Stable localized pulse with* $q = 3.25$, $\lambda = -.2$, $c_1 = 1$. *Grey scale indicates magnitude of* $u_j(t)$. *Index is horizontal, and time runs vertically from* 0 *to* 10. (B) *Pulse width versus* q. *Inset shows* r_j^2, *which appears to be stationary. The horizontal line at* 1 *shows the points at which the width is measured.*

This makes the pulses here quite different from those described in models for working memory (see the discussion and the next section), which have aperiodic behavior. As the parameter q decreases, the width of the pulses gets larger (Figure 5(B)). We conjecture that the width goes to infinity as $|q|$ decreases to q_∞. Figure 3 indicates that the velocity of the fronts goes to zero as q goes to a critical value, q_0. We conjecture that $q_\infty = q_0$, and for the present system that this critical value of q is around 2.5. The reason for this is as follows. Suppose that $q < q_\infty$. Then there are no finite-width pulses. That is, an initial stimulus in the middle of the medium will expand without bound. This is just a pair of wavefronts propagating outward. Similarly, if $q > q_0$, then there are no waves with a positive velocity; we expect that localized sufficiently large initial data will persist and not propagate.

3.5.3. Interactions of pulses. It is possible to initiate multiple pulses in the same medium; however, the behavior is quite dependent on the initial distance as well as the relative phases of the two initial conditions. For example, it is possible for two pulses to merge and form a single pulse, or they can merge and then expand to fill the medium. In the following simulations, the medium is started at rest except for two local regions in which u_j is either 1 or -1. When $u_j = 1$ for both regions, we call this an "in-phase" initial condition, and when $u_j = -1$ we call it "out-of-phase." Figure 6 shows some examples. In (A), a pair of in-phase initial data merge and then chaotically fill the medium. This suggests that the appearance of pulses and the steady-state behavior could depend on the amount of medium initially excited. Indeed, if we excite successively larger parts of the medium, there is a transition from

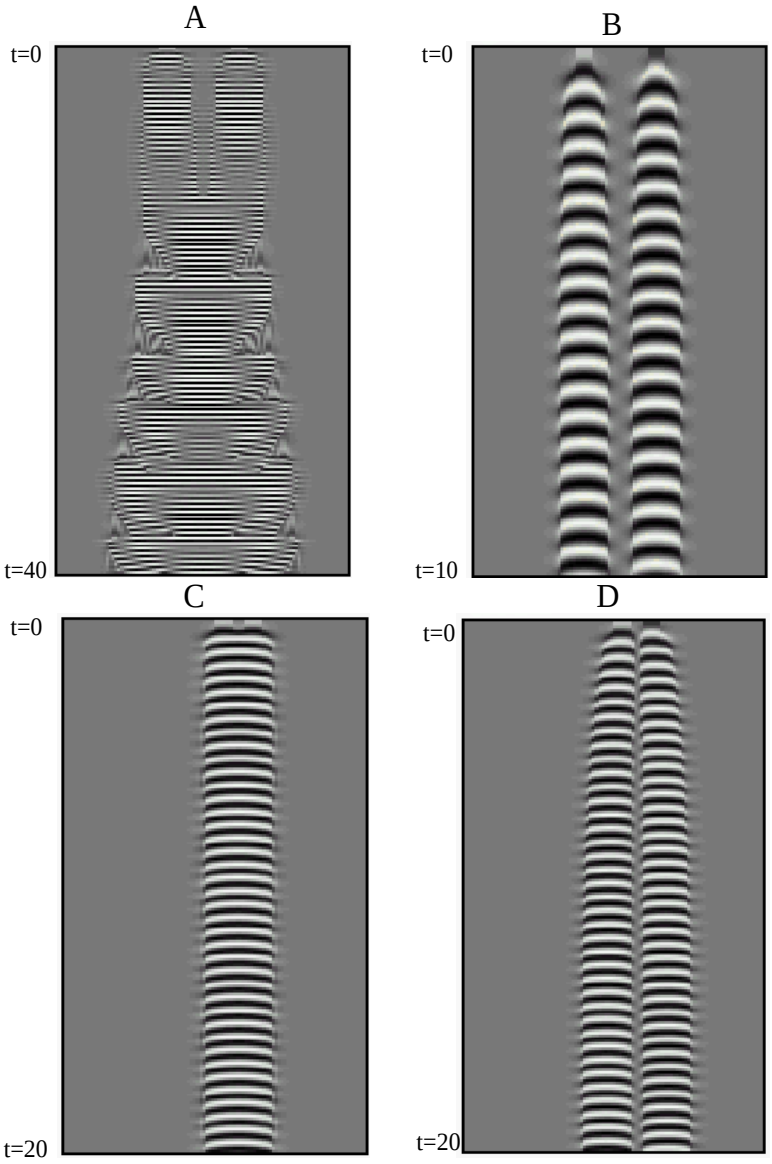

FIG. 6. *Interactions between pulses.* (A) *Two initiated in-phase lead to chaotic behavior;* (B) *same as* (A) *but initially out of phase;* (C) *same as* (A) *but started closer together, leading to merging;* (D) *two out-of-phase pulses split apart. All figures have* $q = 3.25, c_1 = 1, \lambda = -0.2$.

spatially localized behavior to chaotically expanding behavior. In Figure 6(B), the same initial data are given as in A, but the two are out of phase. This results in a pair of local pulses oscillating exactly a half-cycle out of phase. In Figure 6(C), an in-phase pair is started close to each other, leading to simple merging to a single pulse. Finally in (D), the same initial data as in (C) but in antiphase results in a splitting apart of the two pulses rather than a merging. There are many other aspects of interaction which remain to be explored. In particular, the transition between localized pulses and slow chaotic spreading is an intriguing problem.

4. Conductance-based models. The results described in the previous section apply to a very special system of equations, namely, the normal form for a Hopf bifurcation. Thus, a natural question to ask is whether a system away from the bifurcation can have the same behavior. In this section, we consider the behavior of a simple biophysical model with synaptic coupling. The Morris–Lecar (ML) model [21] is a membrane model with leak, calcium, and potassium currents. With the right choice of parameters, the isolated model undergoes a subcritical Hopf bifurcation and has a small regime of bistability between a resting state and a periodic solution. Thus, we will synaptically couple an array of ML neurons and, by altering the applied current, show that the network is able to produce both traveling fronts joining a fixed point to a periodic orbit and localized regions of activity. The equations for each cell are

$$\begin{aligned} C\frac{dV}{dt} &= I - g_l(V - E_l) - g_{Ca}m_\infty(V)(V - E_{Ca}) - g_K n(V - E_K) - I_{syn}, \\ \frac{dn}{dt} &= \frac{n_\infty(V) - n}{\tau_n(V)}, \\ \frac{ds}{dt} &= \alpha(V)(1 - s) - \frac{s}{\tau}, \end{aligned} \tag{4.1}$$

where I_{syn} is the total synaptic current applied to the ith neuron:

$$I_{syn,i} = \left(\sum_j W(i-j)s_j \right) (V_i - E_{syn}).$$

The functions and parameters used are in the appendix. Basically the g's are maximal conductances, the E's are reversal potentials, and $W(j)$ is the coupling strength between neurons and decays with distance. In the normal form, we are able to alter certain abstract parameters such as the imaginary part of the coupling and the nonlinear frequency parameter q. In the actual model, there is no direct analogue of these parameters. However, we can instead alter the applied current I to take the system into and out of the regime of bistability. In Figure 7, we choose I so that the network is near the onset of spontaneous periodicity but remains bistable. A shock at the left of the medium results in a propagating wave shown on the left. Decreasing the current (and making the network less excitable) results in a pulse.

Unlike in the simplified model, the pulse does not seem to be periodic. Rather, it is aperiodic, as is often the case for conductance-based models (see, e.g., [18]).

5. Discussion. We have used a simple canonical model of a bistable oscillatory system to study the propagation of periodic waves and the loss of these waves as either the threshold (λ) changes or the "twist"(q) varies. We have also studied the stability of plane waves in this system. In previous work, we have shown that diffusive coupling in a bistable (oscillatory and fixed point) system leads to a unique traveling front [9]. We also showed that as the threshold changed, the waves disappeared, leaving in their wake spatial patterns. Similar behavior is found in the present model. Unlike the results in [9], we have no closed form for the traveling waves. The existence of wavefronts for sufficiently small values of q remains an open problem; we have proved it only for $q = 0$.

The physiological motivation for this work comes from the behavior of disinhibited slices of cortical tissue [11, 5]. Shocking the tissue results in the propagation of a front

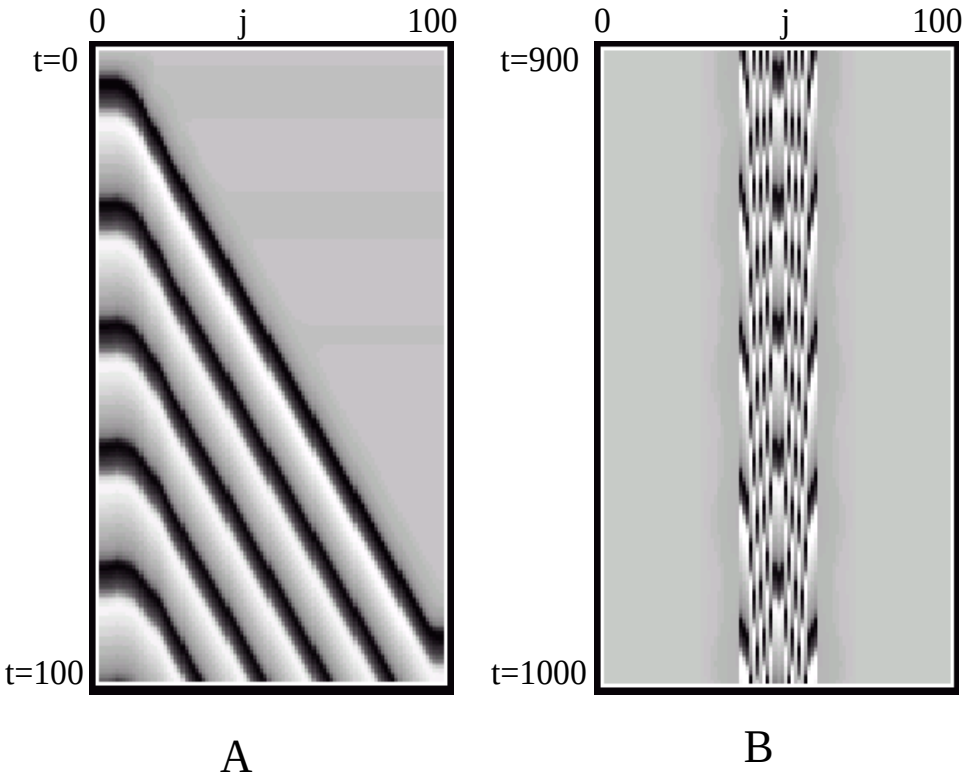

FIG. 7. *Evolution of the voltage for a network of* 100 *ML neurons. The horizontal axis is cell number, and the vertical axis is time in milliseconds. White is a potential of* -45 *mV, and black is a potential of* 20 *mV.* (A) *Traveling wave for* $I = 88$. (B) *Localized pulse for* $I = 82$.

of activity. In experiments the activity eventually terminates due to additional slow processes so that, rather than a front, one obtains a traveling pulse with a finite number of oscillations within the envelope. The present model can be augmented by the addition of a slow negative feedback term, which will terminate the activity, resulting in a spatially confined propagating pulse.

Stationary patterns of localized activity in networks of spiking models have been suggested as models for locally persistent neural activity known as working memory [18, 22]. In these models, the mechanism depends on recurrent excitation of the neurons coupled with *lateral inhibition*. In the context of these models, lateral inhibition means that the connection function $J(x)$ is positive for small $|x|$ and negative for $|x|$ sufficiently large. The present model provides another mechanism which does not depend on lateral inhibition. Rather it depends on bistability between an oscillatory and a rest state. [3] utilized bistability in a firing rate model to obtain localized structures, but, as in the above-mentioned models, they require lateral inhibition. The reason for this can be clarified by looking at our model without the oscillatory component:

$$r_t = r(\lambda + br^2 - r^4) + c\int_{-\infty}^{\infty} J(x-y)r^3(y,t)\ dy.$$

The results of [4], while not precluding localized structures, indicate that in the bistable case, the main type of behavior observed will be stable traveling fronts.

Thus, even though the system is bistable, localized pulses cannot be found with positive $J(x)$. However, the presence of oscillations enables local phase gradients to develop, which can prevent the expansion of the wavefronts beyond a certain range. The mechanism applies to whole classes of voltage-dependent models in which there is a subcritical Hopf bifurcation as current is applied to the system (so-called Type II excitability; see [21]).

It still remains to rigorously prove the existence of these stationary solutions. These satisfy

$$0 = R(\lambda + b_1 R^2 - R^4) + c_1 \int_{-\infty}^{\infty} J(x-y) R^3(y) \cos[\Theta(y) - \Theta(x)]\ dy,$$
$$R(x)\Omega = qR^3(x) + c_1 \int_{-\infty}^{\infty} J(x-y) R^3(y) \sin[\Theta(y) - \Theta(x)]\ dy,$$

where Ω is an unknown parameter, $R(\pm\infty) \to 0$, and $\Theta(0) = 0$. In the case in which $J(x) = \exp(-|x|)/2$, one can then convert the integral equations to a set of differential algebraic equations as follows. Let

$$C(x) = \int_{-\infty}^{\infty} J(x-y) R^3(y) \cos(\Theta(y))\ dy,$$
$$S(x) = \int_{-\infty}^{\infty} J(x-y) R^3(y) \sin(\Theta(y))\ dy,$$

so that we must solve

$$C - C_{xx} = R^3(x) \cos\Theta(x), \qquad S - S_{xx} = R^3(x) \sin\Theta(x),$$

with the constraints

$$0 = R(\lambda + b_1 R^2 - R^4) + c_1 \left(\cos\Theta(x) C(x) + \sin\Theta(x) S(x)\right),$$
$$R\Omega = qR^3 + c_1 \left(\cos\Theta(x) S(x) - \sin\Theta(x) C(x)\right).$$

We have made little progress on this open problem.

Appendix. In the ML equations (4.1), V denotes membrane potential, C is membrane capacitance, and m and h are gating variables. The g's and E_j's are the maximal conductances and reversal potentials, respectively, for calcium, potassium, and leak currents. The gating functions are as follows:

$$n_\infty(v) = .5\left(1 + \tanh\left(\frac{v - v_3}{v_4}\right)\right),$$

$$m_\infty(v) = .5\left(1 + \tanh\left(\frac{v - v_1}{v_2}\right)\right),$$

$$k(v) = \frac{1}{1 + \exp\left(-\dfrac{v - v_t}{v_s}\right)},$$

$$\tau_n(v) = \frac{1}{\cosh\left(\dfrac{v - v_3}{2v_4}\right)},$$

where $v_t = 10$, $v_s = 5$, $v_1 = -1.2$, $v_2 = 18$, $v_3 = 2$, and $v_4 = 30$.

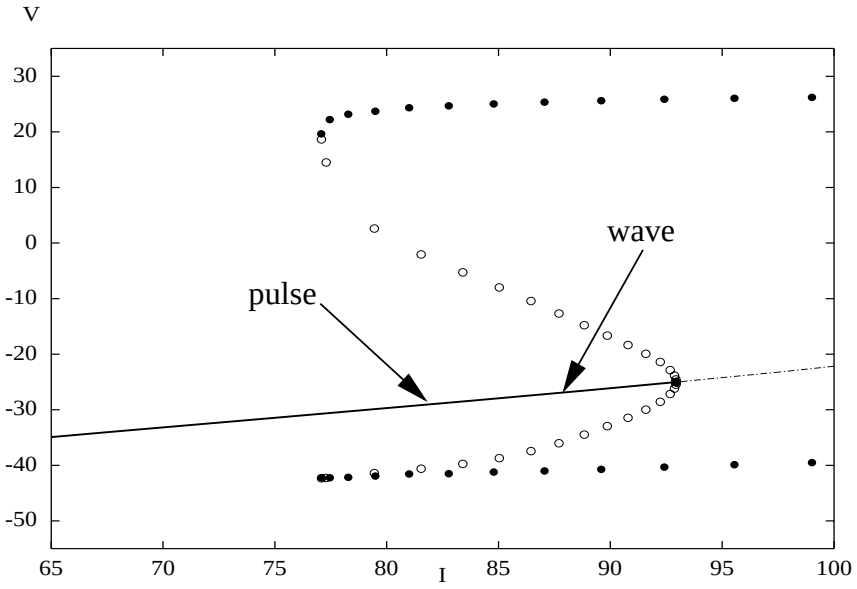

FIG. 8. *Bifurcation diagram obtained by varying I. Arrows denote the values of the current used for the wave and pulse shown in Figure 7.*

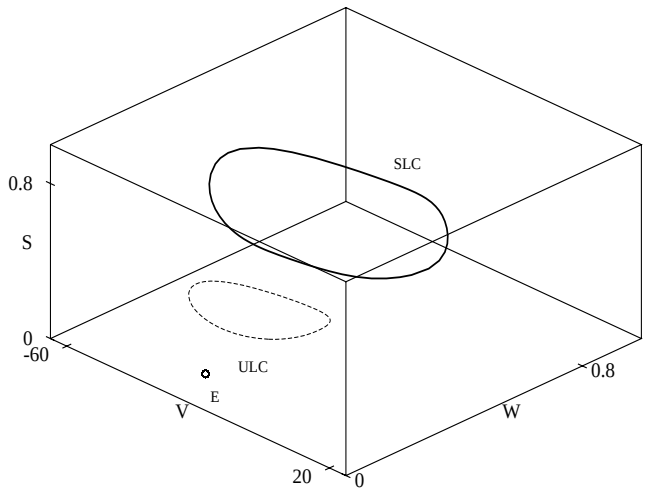

FIG. 9. *In this figure, ULC is the unstable periodic orbit separating the stable fixed point (E) and the stable periodic solution (SLC) in three dimensions (V, w, s) for the ML model.*

The parameters for the ML equations (4.1) for Figure 7 are $\phi = .16$, $g_l = 2$, $g_{ca} = 4.4$, $g_k = 8$, $E_K = -84$, $E_L = -60$, $E_{Ca} = 120$, $E_{syn} = 0$, $\tau_{syn} = 50$, $\alpha = 1$, $g_{syn} = 0.3$, and $C = 5$. With these parameters, the Hopf bifurcation that causes the bistability occurs slightly to the right of $I = 93$. The current used for the traveling waves is $I = 88$ and for the pulses, $I = 82$. These are indicated in the bifurcation diagram. From the bifurcation diagram in Figure 8, at the chosen values for I there

is a stable rest state and a stable periodic, separated by an unstable separatrix. A picture of these orbits is shown in Figure 9. It is not easy in three dimensions to delineate the basins of attraction for the two stable orbits; however, we have found that low values of s and (V, w) near the fixed point are pulled into the rest state, while all other initial data are attracted to the limit cycle.

From the bifurcation diagram, it is possible to estimate the parameters $\lambda = 11.07$, $b = 0.56$, $q = 2.47$ for the model. (Note that we have converted the timescale from milliseconds to seconds, since frequencies are typically measured in Hz.)

REFERENCES

[1] D.G. Aronson, G.B. Ermentrout, and N. Kopell, *Amplitude response of coupled oscillators*, Phys. D, 41 (1990), pp. 403–449.

[2] P.C. Bressloff and S. Coombes, *A dynamical theory of spike train transitions in networks of integrate-and-fire oscillators*, SIAM J. Appl. Math., 60 (2000), pp. 820–841.

[3] M. Camperi and X.-J. Wang, *A model of visuospatial short-term memory in prefrontal cortex: Cellular bistability and recurrent network*, J. Comput. Neurosci., 5 (1998), pp. 383–405.

[4] X. Chen, *Existence, uniqueness, and asymptotic stability of traveling waves in nonlocal evolution equations*, Adv. Differential Equations, 2 (1997), pp. 125–160.

[5] Z. Chen and B. Ermentrout, *Wave propagation mediated by $GABA_B$ synapse and rebound excitation in an inhibitory network: A reduced model approach*, J. Comput. Neurosci., 5 (1998), pp. 53–69.

[6] E. Doedel, *AUTO: A program for the automatic bifurcation analysis of autonomous systems*, Congr. Numer., 30 (1981), pp. 265–284.

[7] G.B. Ermentrout, *Stable small amplitude solutions in reaction-diffusion systems*, Quart. Appl. Math, 39 (1981), pp. 61–86.

[8] B. Ermentrout, *Type* I *membranes, phase resetting curves, and synchrony*, Neural Comput., 8 (1996), pp. 979–1001.

[9] B. Ermentrout, X. Chen, and Z. Chen, *Transition fronts and localized structures in bistable reaction-diffusion equations*, Phys. D, 108 (1997), pp. 147–167.

[10] B. Ermentrout and M. Lewis, *Pattern formation in systems with one spatially distributed species*, Bull. Math. Biol., 59 (1997), pp. 533–549.

[11] D. Golomb and Y. Amitai, *Propagating neuronal discharges in neocortical slices: Computational and experimental study*, J. Neurophysiol., 78 (1997), pp. 1199–1211.

[12] M. Golubitsky and D.G. Schaeffer, *Singularities and Groups in Bifurcation Theory*, Vol. I, Appl. Math. Sci. 51, Springer-Verlag, New York, 1985.

[13] F.C. Hoppensteadt and E.M. Izhikevich, *Weakly Connected Neural Networks*, Springer-Verlag, New York, 1997.

[14] E.M. Izhikevich, *Class* 1 *neural excitability, conventional synapses, weakly connected networks, and mathematical foundations of pulse-coupled models*, IEEE Trans. Neural Networks, 10 (1999), pp. 499–507.

[15] E.M. Izhikevich, *Neural excitability, spiking, and bursting*, Internat. J. Bifur. Chaos, 10 (2000), pp. 1171–1266.

[16] E.M. Izhikevich, *Subcritical elliptic bursting of Bautin type*, SIAM J. Appl. Math., 60 (2000), pp. 503–535.

[17] Yu. A. Kuznetsov, *Elements of Applied Bifurcation Theory*, Springer-Verlag, New York, 1998.

[18] C. Laing and C.C. Chow, *Stationary bumps in networks of spiking neurons*, Neural Comput., 13 (2001), pp. 1473–94.

[19] Y. Loewenstein and H. Sompolinsky, *Oscillations by symmetry breaking in homogeneous networks with electrical coupling*, Phys. Rev. E, 65 (2002), paper 51926.

[20] M.I. Rabinovich, A.B. Ezersky, and P.D. Weidman, *The Dynamics of Patterns*, World Scientific, London, 2000.

[21] J. Rinzel and B. Ermentrout, *Analysis of neural excitability and oscillations*, in Methods in Neuronal Modeling: From Ions to Networks, C. Koch and I. Segev, eds., MIT Press, Cambridge, MA, 1998, Chapter 7, pp. 251–291.

[22] X.-J. Wang, *Synaptic basis of cortical persistent activity: The importance of NMDA receptors to working memory*, J. Neurosci., 19 (1999), pp. 9587–9603.

[23] S. Wiggins, *Introduction to Applied Nonlinear Dynamical Systems and Chaos*, Springer-Verlag, New York, 1990.